33rd Annual International Conference of the IEEE EMBS
Boston, Massachusetts USA, August 30 - September 3, 2011

Detecting changes in human motion using stochastic distance measures

Muhammad Choudry, Matthew Pillar, Tyson Beach, Dana Kulić, and Jack P. Callaghan

Abstract — **We propose a stochastic framework to analyze and compare differences in human motions for applications in injury prevention, rehabilitation, sports training and performance research. Human motions are modeled as Hidden Markov Models and the differences between the motions are measured using the Kullback-Leibler distance metric. The distance metric is recomputed with degrees of freedom excluded to determine which degree of freedom most influences the difference between a set of motions. The proposed system is tested on a human motion dataset consisting of lifting movements under differing load weights and ankle bracing conditions. Results indicate that the algorithm is capable of successfully determining which joints are impacted and ranking them according to importance.**

I. Introduction

Given that personal movement patterns can influence injury, rehabilitation, and performance outcomes [1], there exists a need for methods which can objectively classify and detect differences in motion exhibited between individuals and over time. Methods that are also capable of identifying relative contributions of specific body segments or joint motions to differences in whole body movements are particularly desirable because this information can be used to better understand the implications of inter- and intra-individual variations in movement and to develop and evaluate intervention strategies. In this paper we propose an automated framework utilizing a stochastic representation of motion to quantitatively measure how much each joint contributes to the difference between two whole body motions.

Recently there has been an increased interest in applying artificial intelligence techniques to automate and improve the analysis of human motions [2]. Such techniques include Support Vector Machines (SVM) [3,4], Artificial Neural Networks (ANN) [5,6], decision trees [7], and Hidden Markov Models (HMM) [8,9]. Typically when SVMs, ANNs, and decision trees are used to compare motions certain features from the time series motion data are selected as the basis for comparison. The classification accuracy of these methods relies on selecting the correct set of features. Abstracting a motion to a set of features results in a loss in temporal information and variance in the motions is typically treated as noise due to the deterministic nature of these algorithms. It has been argued convincingly, however, that movement variability is an important and commonly observed feature of human performance that should not always be treated as noise by movement scientists [10].

In comparison, an HMM [11] is a stochastic representation of the movement that captures the variability of motions that appear over several demonstrations, in addition to capturing the temporal information describing the movement progression.

We propose a novel framework for comparing motions based on an HMM representation. Similar to the approach of Kulić et al. [9], the Kullback-Leibler (KL) distance [11], a measure of dissimilarity between models, is used to compare two motion models. In the proposed framework, Degrees of Freedom (DOF) are excluded from the trained model in order to determine how that DOF affects the difference between two motions. The system then ranks the DOF in terms of similarity between the motions. We tested our system on a human motion dataset in which subjects performed laboratory-simulated occupational lifting tasks with and without their right ankle immobilized.

II. Motion Analysis Framework

A. Motion Representation

When performing human motion analysis, different signal sets can be considered, including: joint angle, Cartesian coordinates, or EMG data. Our framework is general and allows the use of any one of, or a combination of, these signals. HMMs [11] are used to model each movement.

Every HMM λ is composed of three main parameters:

$$\lambda = (\pi, A, B) \quad (1)$$

where π is the initial probability vector, A is the transition matrix and B is the probability distribution function. Left-to-right HMM models are used, so that $\pi_1 = 1$. Elements of the transition matrix A are defined as:

$$a_{ij} = P\{q_t = S_j | q_{t-1} = S_i\}, \quad a_{ij} \geq 0, \quad \sum_{j=1}^{N} a_{ij} = 1 \quad (2)$$

where a_{ij} is the probability that the model will transition to state S_j at time t given that the model was previously at state S_i at time t-1. For the observation probability distribution B we use multivariate Gaussian distributions:

$$b_i(\bar{O}) = \mathcal{N}_K(\mu_i, U_i) \quad (3)$$

Where b_i is the observation probability function of state S_i, $\bar{O}$ is the observation vector generated by state S_i, and $\mathcal{N}_K$ is a K-dimensional Gaussian consisting of the mean vector μ_i and the covariance matrix U_i.

To construct a model, parameters for λ are initialized and trained based on a set of observation sequences, using equal

Muhammad Choudry, Matthew Pillar, and Dana Kulić are with the Department of Electrical and Computer Engineering, University of Waterloo, 200 University Avenue West, Waterloo, Ontario, Canada.

Tyson Beach and Jack P. Callaghan are with the Department of Kinesiology, University of Waterloo, 200 University Avenue West, Waterloo, Ontario, Canada.

state initialization as proposed in [12] and the Baum-Welch training algorithm [11].

B. General Comparison of Motions

To compare HMM models the Kullback-Leibler (KL) distance [11] is used:

$$D(\lambda_1,\lambda_2) = \frac{1}{T}\left[\log P\left(O^{(2)}|\lambda_1\right) - \log P\left(O^{(2)}|\lambda_2\right)\right] \quad (4)$$

where $O^{(2)}$ is an observation sequence generated from λ_2, $P(O|\lambda)$ is the probability that an observation sequence O was generated by the model λ, and T is the length of the observation sequence. An efficient algorithm for computing $P(O|\lambda)$ is the forward algorithm [11].

The KL distance is non-symmetric [11]. To obtain a symmetric measure we calculate the symmetric distance D_s using the following relationship:

$$D_s(\lambda_1,\lambda_2) = \frac{D(\lambda_1,\lambda_2) + D(\lambda_2,\lambda_1)}{2} \quad (5)$$

C. Degree-of-Freedom Comparison of Motions

In this section we introduce our proposed method for comparing motions and determining the sources of variation.

Initially individual HMM models are trained for each motion. To compare the difference in a DOF between two motion models λ_1 and λ_2, the mean and covariance for that DOF is removed from the model. Then the distance between λ_1 and λ_2 is computed with the DOF excluded. This is repeated for all the DOF's in λ_1 and λ_2. When comparing these distances, the excluded DOF that results in the smallest distance is the DOF that separates the two motions the most.

Let us now formalize the procedure for this analysis. Given a set of T trained models denoted as:

$$\lambda = \{\lambda_1, \lambda_2, \lambda_3, \ldots \lambda_T\} \quad (6)$$

For each model we have training observation sequences (i.e. recorded data) for F number of DOFs:

$$O = \{o_1, o_2, o_3, \ldots o_F\} \quad (7)$$

Then each model λ_i is a function of O such that:

$$\lambda_i(o_i) = \lambda_i(\{o_{i1}, o_{i2}, o_{i3}, \ldots o_{iF}\}) \quad (8)$$

Next the DOF e is excluded from the model such that λ_i becomes the model $\lambda_{i,e}$ with excluded DOF e:

$$\lambda_{i,e}(o_{ie}) = \lambda_i(\{o_{i1}, o_{i2}, \ldots o_{i,(e-1)}, o_{i,(e+1)} \ldots o_{iF}\}) \quad (9)$$

Note that the DOF information is excluded by removing the e^{th} element in all μ vectors and removing the e^{th} rows and columns from all U matrices that constitute B for the model λ_i.

Now we can calculate the distance vector D_E comparing excluded DOF models for λ_i and λ_j as:

$$D_E(\lambda_i,\lambda_j) = \begin{pmatrix} D_s(\lambda_{i1},\lambda_{j1}) \\ D_s(\lambda_{i2},\lambda_{j2}) \\ \vdots \\ D_s(\lambda_{iF},\lambda_{jF}) \end{pmatrix} = \begin{pmatrix} d_{ij1} \\ d_{ij2} \\ \vdots \\ d_{ijF} \end{pmatrix} \quad (10)$$

The next step is to order the values in the vector $D_E(\lambda_1,\lambda_2)$ by magnitude, where the smallest distance number will correspond to the DOF that most impacts the difference between the two motions.

D. Joint Comparison of Motions

The method in II-C considers the contribution of each individual DOF to the difference between motions, but we may also be interested in analyzing the contribution to groups of DoFs, for example for those joints which are multi DOF, such as the hip or shoulder. In this case the procedure is modified to exclude sets of 3 DOF. We define a joint as a set of 3 DOF (consisting of either x, y, z in Cartesian coordinates or θ, φ, ψ in Cardan joint angles).

Equation 9 is modified such that when a set s is excluded (where $0 \le s \le F/3 - 1$) from the motion λ_i it becomes the excluded set model $\lambda_{i,s}$:

$$\lambda_{i,s}(o_{i,(s*3+1)}\, o_{i,(s*3+2)}\, o_{i,(s*3+2)}) = \lambda_i(\{o_{i1}, o_{i2}, \ldots o_{i,(s*3)}, o_{i,(s*3+4)} \ldots o_{iF}\}) \quad (11)$$

Next the D_E vector in equation 10 is modified to account for computation of F/3 distance calculations instead of F distance calculations:

$$D_E(\lambda_i,\lambda_j) = \begin{pmatrix} D_s(\lambda_{i1},\lambda_{j1}) \\ D_s(\lambda_{i2},\lambda_{j2}) \\ \vdots \\ D_s(\lambda_{iF/3},\lambda_{jF/3}) \end{pmatrix} = \begin{pmatrix} d_{ij1} \\ d_{ij2} \\ \vdots \\ d_{ijF/3} \end{pmatrix} \quad (12)$$

III. Experimental Procedure

A. Experiment Setup

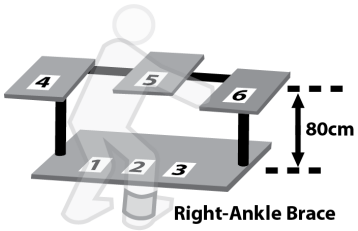

Figure 1 - Configuration Setup: Lift Origins (1,2,3) and Destinations (4,5,6) are Labeled

The data used to test our approach was collected in an experiment examining the influence of unilateral ankle immobilization on low-back loading and injury potential during lifting [13]. Using an optoelectronic motion capture system (Optotrak Certus, NDI, Waterloo, Canada), the positions and orientations of the feet, shanks, thighs, pelvis, and trunk of 10 male subjects were captured while they performed lifting tasks. A 24 DOF Cartesian model was used. Standard inverse kinematics computations were used to convert the positions into Cardan joint angles for the ankles, knees, hips, and lumbar spine. The joint angles formed a 21 DOF joint-angle model.

With and without their right ankle immobilized, subjects lifted two masses (light = 3.7 kg; heavy = 12.7 kg) from three different origins (positions 1, 2, and 3) to three different destinations (4, 5, and 6) (figure 1). Three repetitions of each task were performed. Ankle immobilization was achieved through the use of a brace designed to restrict ankle motion in all three anatomical planes.

B. HMM Model Configuration Details

A model was trained for each combination of: Cartesian / joint angle representation, movement task, loading condition, and bracing condition. Only the trajectory data from the start of the load lifting to the end of the load release was considered. Prior to training, the trajectory data for each individual DOF was normalized on the range from -1 to 1 using the minima and maxima of the DOF trajectory across all subjects.

All motion primitives were modeled as 15 state HMMs. The optimum number of states for the models was determined with Leave-One-Out Cross Validation.

The covariance matrices were modeled as diagonal matrices, due to the limited size of the training data set (30 data sets per motion).

IV. Results And Discussion

Analyses were conducted on the full dataset described in section III-A, but for brevity only a subset of the results are presented here to demonstrate the utility of the proposed methodology. Summarized in figure 2 are findings from the general level comparisons; results from selected joint level comparisons are presented in figures 3 and 4.

Regardless of whether motions were modeled using Cartesian coordinates or joint angles in the general-level comparisons, the distance measures for a motion subgroup (i.e. same motion under various constraints) typically clustered around a certain mean distance number (figure 2). Thus it is possible to distinguish between motions on the basis of the distance metric. Looking at the joint angle representation we see that the distance numbers for a specific motion sub-group tended to form clusters with a smaller standard deviation in comparison to the Cartesian representation. This tells us that for this dataset the joint angle data may be better for differentiating between different motion types and that Cartesian data may contain additional information for analyzing variations within a motion subgroup. Note that distances in figure 2 have been normalized to account for the different number of DOF in the Cartesian and joint-angle data by dividing the distances by the number of DOF.

In figure 2, distances within each motion sub-group are compared to see the impact of the constraints. For example in motions 3to4 we found that 'light and no brace motion' was most similar to the 'heavy and no brace' motions and that 'heavy and brace' motion was the most dissimilar to the 'light and no brace' motion. This is expected since the similar motion had one constraint changed where as the most dissimilar motion had two constraints changed.

Next we identified the specific sources of differences in motions 3to4 at the joint level (section II-D). The excluded joint that resulted in the smallest distance has the most impact on the motion difference. In agreement with the previously reported findings of the original experiment [13], figures 3-a and 3-c show that the right ankle joint was affected most by the brace. Results from the Cartesian coordinate dataset were also consistent with these findings, as the right shank was the segment most impacted by right ankle immobilization (figures 4-a and 4-c). This makes sense as changes in Cartesian coordinates of the right shank are affected by position of the right ankle joint.

Beach et al. also found that under braced conditions, there was a tendency for subjects to exhibit greater spine flexion to compensate for the loss of ankle mobility [13]. While this tactic is not apparent in the joint angle distances, the Cartesian data resulted in relatively lower distance numbers for the trunk indicating that this is one of the body parts that exhibited different movement between the braced and non-braced motions. Perhaps the reason the joint angle data set did not similarly characterize this response was because between-condition differences in spine flexion (~ 2-5 degrees) were not statistically significant across all lifting tasks [13].

Next we were interested in finding new trends that were not observed in [13]. In figures 3-b and 4-b it can be seen that in the joint angle representation, the left ankle and trunk were impacted the most by the size of load lifted. In the Cartesian representation, the pelvis and trunk were impacted the most by load. We noted that motion 3to4 in particular requires shifting the weight of the body on to the left foot and we also expected that lower back motion would be affected by lifting a heavier weight. Our results were later confirmed by Beach et al in [14], a continuation of the study [13], where they found that the motion (about all anatomical axes) of the left ankle was significantly affected by load ($p < 0.0036$) and the angle of the trunk (with respect to the pelvis) was significantly affected by load about two axes.

V. Conclusions And Future Work

This paper proposes an approach for detecting changes in motions by using stochastic models to represent time series movement data. This allows us to capture the temporal and spatial variability inherent in human motions. Our method allows the use of joint angle, Cartesian coordinates, or EMG data, and any combination of these signals for analysis. We present an approach for analyzing the change in individual DOF and joints wherein we excluded specific DOF information from trained HMM models to detect the change in the motion. By finding the minimum KL distance between excluded DOF models we were able to find out which DOF was most affected by motion constraints. This approach for analyzing DOF is suitable for automatically finding changes in signals for a high DOF data set where the location of the change in motion is not known a priori. We tested our framework on a human movement dataset in which subjects lifted loads under various conditions. Our results match those found in a previous study [13]. Thus, our approach shows promise for use in human motion analysis, with potential applications to rehabilitation, sports training and medical diagnosis.

Future work will focus on analyzing the temporal variability of the distances over the duration of the motion as well as detecting common strategies that subjects may try to

use for performing similar motions. In addition to this, the proposed method could be extended to exclude combination of joints in order to determine which set of joints is the most impacted. This would be useful because in human motions limbs tend to move in synchronous manner.

REFERENCES

[1] S. McGill, "Evolving ergonomics?," Ergonomics, No. 52, pp. 80–86, 2009

[2] R. Bartlett, "Artificial intelligence in sports biomechanics: New dawn or false hope?," Sports Science and Medicine No. 5, pp. 474-479, 2006

[3] W. Gilleard et al, "Detecting trunk motion changes due to pregnancy using pattern recognition techniques," Intl. Conf on IEEE EMBS, pp. 2405-2408, 2008

[4] P. Levinger et al, "Support Vector Machines for detecting recovery from knee replacement surgery using quantitative gait measures," Intl. Conf on IEEE EMBS, pp. 4875-4878, 2007

[5] R. Begg and J. Kamruzzaman, "Neural networks for detection and classification of walking pattern changes due to ageing," Australasian Physical & Engineering Sciences in Medicine, Vol. 29, No. 2, pp. 188-195, 2006

[6] J. Perl, "A neural network approach to movement pattern analysis," Human Movement Science, No. 23, pp. 605–620, 2004

[7] A. Salaheldin, M. ElSayed, A. Alsebai, N. El Gayar, M. ElHelw, "Change Analysis for Gait Impairment Quantification in Smart Environments," Int. Conf. on Autonomous and Intelligent Systems , pp. 1-6, 2010

[8] A. Kale, A. N. Rajagopalan, N. Cuntoor, and V. Krueger, "Gait-based recognitions of humans using continuous hmms," in IEEE Int. Conf. on Automatic Face and Gesture Recognition, pp. 336-341, 2002

[9] D. Kulić, G. Venture and Y. Nakamura, "Detecting changes in motion characteristics during sports training," Intl. Conf. on IEEE EMBS, pp. 4011-4014, 2009

[10] R. Bartlett, J. Wheat, and M. Robins, "Is movement variability important for sports biomechanics?," Sports Biomechanics, No. 6, pp. 224–243, 2007

[11] L. R. Rabiner, "A Tutorial on Hidden Markov Models and Selected Applications in Speech Recognition," Proc. of the IEEE, Vol. 77, No. 2, 1989

[12] D. Kulić, W. Takano, and Y. Nakamura, "Incremental Learning, Clustering and Hierarchy Formation of Whole Body Motion Patterns using Adaptive Hidden Markov Chains," IJRR, Vol. 27, No. 7, pp. 761-784, 2008

[13] T. Beach, et al, "Does A Unilateral Restriction in Ankle Mobility Affect Trunk Kinematics and Low-Back Loading During Manual Lifting Tasks?," American Society of Biomechanics Conference, 2009

[14] T. Beach, et al, "Unilateral ankle immobilization alters the kinematics and kinetics of lifting", submitted Spring 2011.

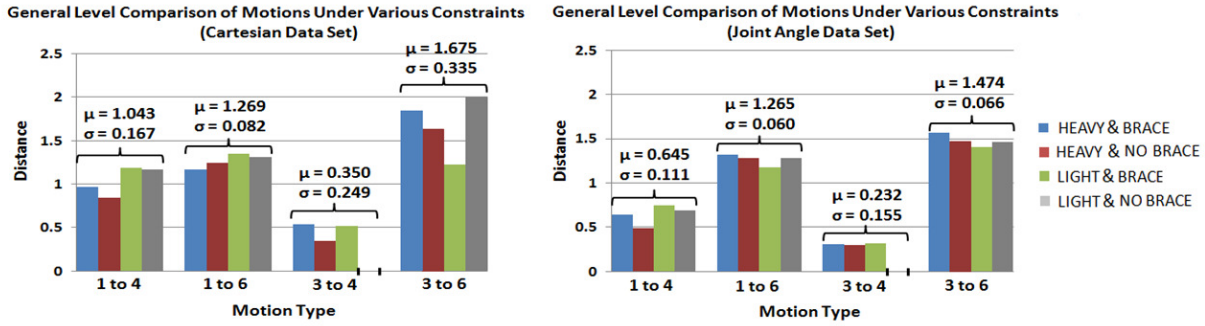

(a) (b)

Figure 2 – General level comparison of motions where distances are with respect to 3to4 'light and no brace'

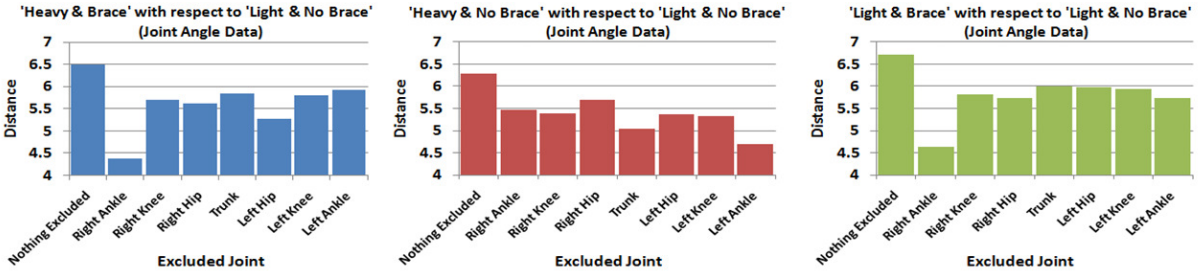

(a) (b) (c)

Figure 3 – Joint level comparison of motions 3to4 using joint angle representation

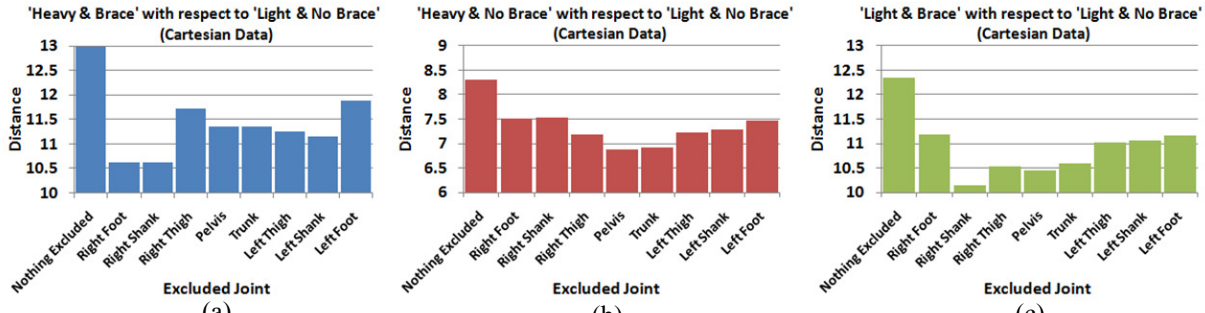

(a) (b) (c)

Figure 4 – Joint level comparison of motions 3to4 using Cartesian representation